

# **Synthesis and Characterization of Ferroelectric ceramic by soft chemical route.**

*A thesis Submitted in partial fulfillment*  
FOR THE DEGREE OF MASTER OF SCIENCE IN PHYSICS  
Under Academic Autonomy  
**NATIONAL INSTITUTE OF TECHNOLOGY, ROURKELA**



**By**

**CHINMAYA MOHAPATRA**

**Under the Supervision of**

**Prof. S. PANIGRAHI**

DEPARTMENT OF PHYSICS  
NATIONAL INSTITUTE OF TECHNOLOGY  
ROURKELA –769008



**NATIONAL INSTITUTE OF TECHNOLOGY**  
**ROURKELA**  
**CERTIFICATE**

This is to certify that the thesis entitled, **“Synthesis and Characterization of ferroelectric ceramic prepared by soft chemical route.”** submitted by Mr. Chinmaya Mohapatra in partial fulfillments for the requirements for the award of Master of Science Degree in Physics Department at National Institute of Technology, Rourkela is an authentic work carried out by him throughout the year under my supervision and guidance.

To the best of my knowledge, the matter embodied in the project has not been submitted to any other University/ Institute for the award of any Degree or Diploma.

Rourkela

Date

Prof S Panigrahi

Department of Physics

National Institute of Technology

## ACKNOWLEDGEMENT

I express my deep sense of gratitude to my supervisor Prof S Panigrahi Dept. of Physics, N.I.T, Rourkela for his valuable guidance and support in carrying out this project. My sincere thanks go to Prof. S. Jena HOD, Physics for providing all kinds of possible help.

I wish to convey my deep felt thanks to Mr V Senthil for his encouragement and support.

I profusely thank all the faculties, office staffs and students of the physics Department, N.I.T Rourkela.

Chinmaya mohapatra

# CONTENT

## Chapter 1: Introduction

1.1:Ferroelectricity

1.2:Perovskite

1.3:Structure of perovskite Barium Titanate( $\text{BaTiO}_3$ )

1.4:Piezoelectricity

1.5: Pyroelectricity

1.6: Ferroelectric Crystal

1.7:Classification of Ferroelectric Crystals

1.7.1: Diffused phase transition

1.7.2: Relaxor Ferroelectricity

## Chapter 2

2.1:Experimental technique

2.1.1:Preparation of Powder Ceramic

2.1.2: Calcinations

2.1.3: Sintering

2.2: Characterization

2.2.1: XRD

2.2.2: DSC

2.2.3: TGA

2.2.4: SEM

2.2.5: Dielectric Study

## Chapter 3

### 3.1: Result and discussion

#### 3.1.1 DSC AND TGA analysis

#### 3.1.2: XRD analysis

#### 3.1.3: SEM

#### 3.1.4: Dielectric Study

#### 3.1.5: PE loop

## Chapter 4: Conclusion

## References

## **List of Figures**

**Fig.1** A cubic ABO<sub>3</sub>, perovskite type unit cell

**Fig.2** Electric field vs polarization loop or P-E loop

**Fig.3** X Ray Diffraction

**Fig.4** . TG and DSC plot of BaTiO<sub>3</sub>

**Fig.5** .XRD pattern of Sr doped BaTiO<sub>3</sub>

**Fig.6** shows the peak shift of Sr doped BaTiO<sub>3</sub>

**Fig.7** . SEM Images of Sr doped BaTiO<sub>3</sub>

**Fig.8** . Frequency dependence dielectric study of Sr doped BaTiO<sub>3</sub> at room temperature

**Fig.9** . Temperature dependence dielectric study of BaTiO<sub>3</sub>

**Fig.10** shows the PE loop of Sr doped BaTiO<sub>3</sub> ceramics at room temperature

## **List of tables**

**Table 1** Table of lattice parameter

**Table 2** Table of  $E_c, P_s, P_r$  values of  $x=0, 0.1, 0.2, 0.4,$

## Abstract

The single phase ceramic powder with general formula  $\text{Ba}_{1-x}\text{Sr}_x\text{TiO}_3$  ceramic is prepared by soft chemical route. The structural analysis was done by XRD. The well defined crystalline XRD pattern was observed with single phase. Upto  $x=0.1$  it is showing tetragonal structure and for higher doping it shows cubic structure. The morphological study was done by SEM which shows that the grain size is effected by the substitution level. The temperature and frequency dependency dielectric study was done. It shows that the dielectric constant at room temperature first increases upto  $x=0.3$  and then decreases for the higher composition. The temperature dependency dielectric study of  $x=0.0$  show a normal ferroelectric behaviour. The ferroelectric behaviour is again confirmed by the P-E loop study.

# Chapter-1

## Introduction

### 1.1 Ferroelectricity

It is the phenomenon in which spontaneous polarization occurs in certain nonconducting crystals material below certain temperature called curie temperature in the absence of an electric field. It is thus analogous to ferromagnetism which represents the state of spontaneous magnetization of the material. Reversing the external field reverses the predominant orientation of the ferroelectric domains, though the switching to a new direction lags somewhat behind the change in the external electric field. This lag of electric polarization behind the applied electric field is ferroelectric hysteresis, named by analogy with ferromagnetic hysteresis. Ferro electricity is named by analogy with ferromagnetism, which occurs in such materials as iron. Iron atoms, being tiny magnets, spontaneously align themselves in clusters called ferromagnetic domains, which in turn can be oriented predominantly in a given direction by the application of an external magnetic field. There are certain crystals showing ferroelectric properties these crystals are called ferroelectric crystals. In such crystals, the centres of positive and negative charges do not coincide with each other even in the absence of electric field, thus producing a non-zero value of the dipole moment.

Ferro electricity was discovered in 1921 by J. Valasek. He discovered that the polarization of sodium potassium tartarate tetra hydrate ( $\text{NaKC}_4\text{H}_4\text{O}_6 \cdot 4\text{H}_2\text{O}$ ), better known as Rochelle salt, could be reversed by application of an electric field. So this Rochelle salt first known ferroelectric material. Unfortunately, Rochelle salt loses its ferroelectric properties if the composition is slightly changed, which made it rather unattractive for industrial applications. After that Barium titanate ( $\text{BaTiO}_3$ ) was discovered to be ferroelectric behavior in 1945 by A Von Hippel and is perhaps the most commonly thought of material when one thinks of ferroelectricity.  $\text{BaTiO}_3$  is stable perovskite type, which is one of the fundamental crystal lattice structures. Perovskites form is the most important class of ferroelectric materials. The perfect perovskites structure follows the formula  $\text{ABO}_3$ , where A is a mono- or divalent and B is a tetra- or pentavalent metal.



## 1.2 Pervoskite

The perovskite family includes many titanates used in various electroceramics applications, for example, electronic, electro-optical, and electromechanical applications of ceramics. Barium titanate, perovskite structure, is a common ferroelectric material with a high dielectric constant, widely utilized to manufacture electronic components such as multilayer capacitors (MLCs), PTC thermistors, piezoelectric transducers, and a variety of electro-optic devices. Barium titanate is a dielectric ceramic used for capacitors. It is a piezoelectric material for microphones and other transducers. The spontaneous polarization of barium titanate is about  $0.15 \text{ C/m}^2$  at room temperature and its Curie point is  $120^\circ\text{C}$ .

## 1.3 Structure of perovskite-Barium Titanate ( $\text{BaTiO}_3$ )

The perovskite-like structure, named after the  $\text{CaTiO}_3$  perovskite mineral is a ternary compound of formula  $\text{ABO}_3$  that A and B cations differ in size. It is considered an FCC- derivative structure in which the larger A cation and oxygen together form an FCC lattice while the smaller B cation occupies the octahedral interstitial sites in the FCC array. There is only the oxygen being B cation's nearest neighbour. The structure is a network of corner-linked oxygen octahedra, with the smaller cation filling the octahedral holes and the large cation filling the dodecahedral hole. The unit cell of perovskite cubic structure is shown below.

In Figure, we can see that the coordination number of A ( $\text{Ba}^{+2}$  Barium) is 12, while the coordination number of B ( $\text{Ti}^{+4}$  Titanium) is 6. In most cases, the above figure is somewhat idealized. In fact, any structure consisting of the corner-linked oxygen octahedra with a small cation filling the octahedral hole and a large cation (if present) filling the dodecahedral hole is usually regarded as a perovskite, even if the oxygen octahedra are slightly distorted. Also, it is unnecessary that the anion is oxygen. For example, fluoride, chloride, carbide, nitride, hydride and sulfide perovskites are also classified as the perovskite structures. As a result, we can say that perovskite structure has a wide range of substitution of cations A and B, as well as the anions, but remember that the principles of substitution must maintain charge balance and keep sizes within the range of coordination number.

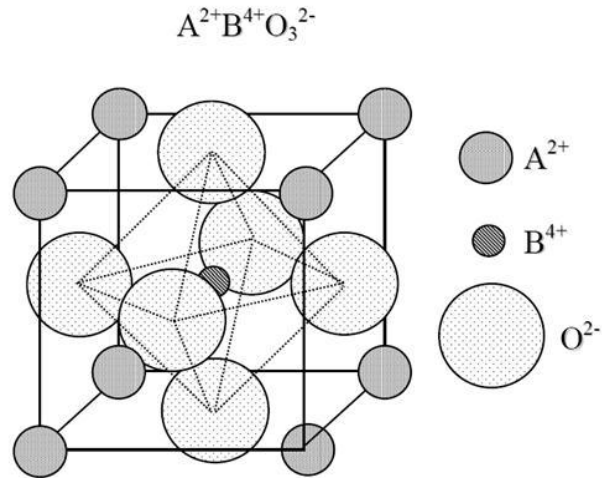


Fig 1. A cubic ABO<sub>3</sub>, perovskite type unit cell

Because the variation of ionic size and small displacements of atoms that lead to the distortion of the structure and the reduction of symmetry have profound effects on physical properties, perovskite structure materials play such an important role in dielectric ceramic.

Structure of BaTiO<sub>3</sub> depends on temperature.

- It shows cubic phase above its curie temperature of about 120<sup>0</sup>C.
- Between 120<sup>0</sup>C and 0<sup>0</sup>C, it shows tetragonal phase
- Between 0<sup>0</sup>C and -90<sup>0</sup>C, it shows orthorhombic phase
- On decreasing the temperature below -90<sup>0</sup>C the phase transition occurs from the orthorhombic phase to rhombohedral phase.

## 1.4 Piezoelectricity

Some materials have the ability to produce electricity when subjected to mechanical stress. This is called the piezoelectric effect. This stress can be caused by hitting or twisting the material just enough to deform its crystal lattice without fracturing it. This is also called direct piezoelectric effect. Piezoelectric materials also show a converse effect, where a geometric strain (deformation) is

produced up on the application of a voltage. The direct and converse piezoelectric effects can be expressed in tensor notation as,

$$P_i = d_{ijk} \alpha_{jk} \text{ (direct piezoelectric effect)}$$

$$\beta_{ij} = d_{ijk} E_k \text{ (converse piezoelectric effect)}$$

$P_i$  is the polarization generated along the  $i$  – axis in response to the applied stress, and  $d_{ijk}$  is the piezoelectric coefficient. For the converse effect,  $\beta_{ij}$  is the strain generated in particular orientation of the crystal up on the application of electric field along the  $k$  – axis.

## 1.5 Pyroelectricity

It is the property of certain crystals to produce a state of electric polarity by a change of temperature. Certain dielectric (electrically nonconducting) crystals develop an electric polarization (dipole moment per unit volume) when they are subjected to a uniform temperature change. This piezoelectric effect occurs only in crystals which lack a center of symmetry and also have polar directions (that is, a polar axis). These conditions are fulfilled for 10 of the 32 crystal classes. Typical examples of pyroelectric crystals are tourmaline, lithium sulfate monohydrate, cane sugar, and ferroelectric barium titanate.

Pyroelectric crystals can be regarded as having a built in or permanent electric polarization. When the crystal is held at constant temperature, this polarization does not manifest itself because it is compensated by free charge carriers that have reached the surface of the crystal by conduction through the crystal and from the surroundings. However, when the temperature of the crystal is raised or lowered, the permanent polarization changes, and this change manifests itself as piezoelectricity. The magnitude of the pyroelectric effect depends upon whether the thermal expansion of the crystal is prevented by clamping or whether the crystal is mechanically unconstrained. In the clamped crystal, the primary pyroelectric effect is observed, whereas in the free crystal, a secondary pyroelectric effect is superposed upon the primary effect. The secondary effect may be regarded as the piezoelectric polarization arising from thermal expansion, and is generally much larger than the primary effect.

Pyroelectrics have a broad spectrum of potential scientific and technical applications. The most developed is the detection of infrared radiation. In addition, pyroelectric detectors can be used to measure the power generated by a radiation source (in radiometry), or the temperature of a remote hot body (in pyrometry, with corrections due to deviations from the blackbody emission). An infrared image can be projected on a pyroelectric plate and transformed into a relief of polarization on the surface. Other potential applications of pyroelectricity include solar energy conversion, refrigeration, information storage, and solid-state science.

## 1.6 Ferroelectric Crystal

A ferroelectric crystal is a crystal which possesses reversible spontaneous polarization as exhibited by a dielectric hysteresis loop (reversibility of the polarization). The uniform polarization region of ferroelectric crystal is called ferroelectric domains. All the dipoles are aligned in same direction within the domain. There may be many domains in a crystal separated by interfaces called domain walls. A ferroelectric single crystal, when grown, has multiple ferroelectric domains. A single domain can be obtained by domain wall motion made possible by the application of an appropriate electric field. A very strong field could lead to the reversal of the polarization in the domain, known as domain switching. All ferroelectric materials are pyroelectric, however, not all pyroelectric materials are ferroelectric. Below a transition temperature called the Curie temperature ferroelectric and pyroelectric materials are polar and possess a spontaneous polarization or electric dipole moment. The non-polar phase encountered above the Curie temperature is known as the paraelectric phase. The direction of the spontaneous polarization conforms to the crystal symmetry of the material, while the reorientation of the spontaneous polarization is a result of atomic displacements. The magnitude of the spontaneous polarization is greatest at temperatures well below the Curie temperature and approaches zero as the Curie temperature is neared.

The most characteristics property of a ferroelectric crystal is the hysteresis loop is shown in (**fig. 2**). As the electric field strength is increased, the domains start to align in the positive direction giving rise to a rapid increase in the polarization. At very high field levels, the polarization reaches a saturation value ( $P_s$ ). The polarization does not fall to zero when the external field is removed. At zero external field, some of the domains remain aligned in the positive direction,

hence the crystal will show a remnant polarization  $P_r$ . The crystal cannot be completely depolarized until a field of magnitude is applied in the negative direction. The external field needed to reduce the polarization to zero is called the coercive field strength  $E_c$ . If the field is increased to a more negative value, the direction of polarization flips and hence a hysteresis loop is obtained. The value of the spontaneous polarization  $P_s$  is obtained by extrapolating the curve onto the polarization axes.

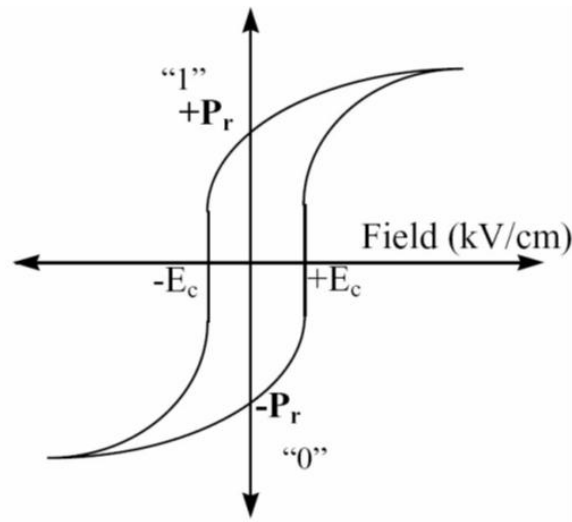


**Fig2.**Electric field vs polarization loop or P-E loop

The relationship between  $P$  and  $E$  is linear up to relatively large fields. However, in the case of ferroelectrics and must be defined more precisely owing to the more complicated relationship between  $P$  and  $E$ . For most purposes of this review, and  $c$  are defined as the slopes of the  $P$  vs.  $E$  curves, at the origin, i.e., the initial values.

$$\epsilon = (\delta d / \delta E)_{E=0} \text{ and } \chi = (\delta P / \delta E)_{E=0} \text{ ----- (1)}$$

They are determined from measurements made at very low ac fields so as not to reverse any domains. Although ferroelectric crystals are a widely varied group, they possess a number of general characteristics properties, among these are the following:

The hysteresis loop disappears at a certain temperature, the Curie point  $T_c$ , above which the crystal behaves as a normal dielectric. It should be noted, however, that in some crystals melting or chemical decomposition may occur before the Curie point is reached.

At  $T_c$  a ferroelectric crystal transforms to a phase of higher symmetry. This higher temperature phase is usually nonpolar, or paraelectric (PE).

The polar crystal structure of a ferroelectric can be derived from the high-temperature PE structure by a slight distortion of the crystal lattice. This is the main reason behind the success of the phenomenological theory of ferroelectricity which assumes that the same free energy function is applicable for both the FE and PE phases.

Ferroelectrics generally have a large  $\epsilon$  (or), which rises to a peak value at  $T_c$ .

Above  $T_c$ ,  $\epsilon$  of a ferroelectric (measured along the polar axis) usually obeys the Curie-Weiss law i.e,

$\epsilon = C/(T - T_0)$ , where  $C$  and  $T_0$  are the Curie-Weiss constant and Curie-Weiss temperature, respectively. Finally, we should mention that there are substances which, on cooling, undergo a transition from a nonpolar to an antipolar state. In this state the crystal has a superlattice consisting of antiparallel dipoles. If, in a given crystal, the coupling energy between these arrays is comparable to that of the polar case, then the crystal is said to be antiferroelectric (AFE). An antiferroelectric crystal can usually be made ferroelectric by the application of a sufficiently large electric field.

## 1.7 Classification of Ferroelectric Crystals

Depending on the temperature variation of dielectric constant or Curie constant  $C$ , ferroelectrics can be divided into two groups. In one group, the compounds undergoing order-disorder type transition, have a Curie constant of the order  $10^3$  while for others which undergoes displacive type transition, it is of the order of  $10^5$ . Initially ferroelectric materials were broadly classified into two categories: (a) soft ( $\text{KH}_2\text{PO}_4$  -type) and (b) hard ( $\text{BaTiO}_3$  -type). The phase transition in soft (H-bonded) ferroelectrics is of order disorder type whereas in hard ones it is displacive type. The phase transition in soft ferroelectrics involves not only the ordering of the disordered

hydrogen atom, but also the deformation of the atomic groups like  $\text{SO}_4^{2-}$ . In case of displacive type of transition a small atomic displacement of some of the atoms is mainly responsible for phase transition, which has been found in some of the perovskites. However, the difference between displacive and order-disorder type of transition becomes uncertain when the separation of relevant disorder becomes comparable with the mean thermal amplitude of those atoms. The character of ferroelectrics is represented in terms of the dynamics of phase transition.

### **1.7.1. Diffuse Phase Transition**

Many phase transitions in macroscopic homogeneous materials are characterized by the fact that the transition temperature is not sharply defined. In these, so-called diffuse phase transition temperature (DPT), the transition is smeared out over a certain temperature interval, resulting in a gradual change of physical properties in this temperature region. Though this phenomenon is observed in several types of materials, however, the most remarkable examples of DPT are found in ferroelectric materials. Ferroelectric diffuse phase transitions (FDPT) are first mentioned in the literature in the early 1950's. Some characteristics of the DPT are: (a) broadened maxima in the permittivity- temperature curve, (b) gradual decrease of spontaneous and remanent polarisations with rising temperature, (c) transition temperatures obtained by different techniques which do not coincide, (d) relaxation character of the dielectric properties in transition region and (e) no Curie-Weiss behavior in certain temperature intervals above the transition temperature. The diffuseness of the phase transition is assumed to be due to the occurrence of fluctuations in a relatively large temperature interval around the transition. Usually two kinds of fluctuations are considered: (a) compositional fluctuation and (b) polarization (structural) fluctuation. From the thermodynamic point of view, it is clear that the compositional fluctuation is present in ferroelectric solids-solutions and polarization fluctuation is due to the small energy difference between high and low temperature phases around the transition. This small entropy difference between ferroelectric and paraelectric phase will cause a large probability of fluctuation. Kanzing has observed from X-ray diffraction that in a narrow temperature range around the transition  $\text{BaTiO}_3$  single crystal splits up into FE and PE micro regions. According to Fritzsche substances of less stability are expected to have a more diffuse transition. For relaxor as well as other FDPT the width of the transition region is mainly important for practical applications.

### 1.7.2. Relaxor Ferroelectricity

High and broad maxima in temperature dependence of both components of complex permittivity  $\epsilon^* = \epsilon - i\epsilon''$  and their shift to higher temperatures with raising measuring frequency is a typical feature of relaxor ferroelectrics (RFEs). Relaxor ferroelectric exhibit many properties similar to those of spin and dipolar glasses. Relaxor behavior is normally FE materials results from compositionally induced disorder or frustration. This behavior has been observed and studied most extensively in disordered  $\text{ABO}_3$  perovskite ferroelectrics and is also seen in mixed crystals of hydrogen-bonded FEs and AFEs, the so-called phonic glasses. In this section we restrict our comments largely to the  $\text{ABO}_3$  oxides. Most of the RFEs with potential piezoelectric applications are lead-based compounds with the perovskite structure; however there is currently an increased need for more environmental friendly lead-free compounds.

In the  $\text{ABO}_3$  oxides substituting ions of different sizes, valences, and polarizabilities at both the A and B lattice sites produces dipolar defects and can introduce a sufficiently high degree of disorder so as to break translational symmetry and prevent the formation of a long-range ordered state. Instead, the dipolar motion in such systems freezes into a glass-like state on cooling below a dynamic transition temperature,  $T_m$ . In these highly polarizable host lattices, the presence of a dipolar impurity on a given site can induce dipoles in a number of adjacent unit cells within a correlation length of that site. We expect the dipolar motion within this correlation length to be correlated, leading to the formation of polar nanodomains. Indeed, such nanodomains have been observed in many  $\text{ABO}_3$  relaxors at temperatures far above the peak in  $\epsilon(T)$ , and their occurrence is now considered to be crucial to the understanding of the properties of relaxors. We picture a distribution of sizes of such nanodomains in which the orientational degrees of freedom are correlated within each domain, but uncorrelated across the various domains. At sufficiently low temperatures, the dipolar motion within each domain freezes, resulting in the formation of an orientation glass (relaxor) state. Such a state is characterized by a distribution of relaxation times related to the sizes of the nanodomains. Two important characteristics of this relaxor state that distinguish it from simple dipolar glasses or spin glasses are the predominant existence of the dipolar nanodomains (vs. largely individual dipoles or spins) and the presence of some degree of cooperative freezing of the orientational degrees of freedom. Evidence of this cooperative effect



comes from the observation of some remanent polarization in electric field hysteresis loops. It should be noted, however, that such evidence is also seen in systems of random dipoles in low polarizability hosts for doped alkali halides with sufficiently high concentration of dipoles.

## Thesis Objective

- To synthesis the high dielectric constant material ( $\text{Ba}_{1-x}\text{Sr}_x\text{TiO}_3$ ) by soft chemical route.
- To characterize the synthesized materials like XRD for phase formation, SEM for surface morphology, P-E loop to show the material is ferroelectric and Electrical study for dielectric constant and transition temperature.

**Motivation:** The discovery of ferroelectricity in barium titanate ( $\text{BaTiO}_3$ ) has given birth to a large number of ABO<sub>3</sub> type materials. The diversity of structures exhibited by  $\text{BaTiO}_3$  based perovskites continues to fascinate in a range of areas including solid state chemistry, physics and the earth science. Ferroelectric oxides with perovskite structure have been currently of great technological interest due to their excellent properties for various related applications in recent years. However it is well known that the ferroelectric materials at present are lead based perovskite that are toxic. Naturally, lead free materials will be of interest because of their obvious health and environmental advantages in future applications. Barium strontium titanate (BST) is a high-K (dielectric constant) material is commonly used to replace silicon dioxide ( $\text{SiO}_2$ ) as the dielectric in advance memory devices. The high dielectric constant combined with a low dissipation factor makes BST one of the promising candidates for dynamic random access memory (DRAM) applications. The tunable dielectric constant results in a change in the phase velocity in the device allowing it to be tuned in real time for a particular application. However, the relatively high loss tangent of these materials, especially at microwave frequencies, has precluded their use in phase shifter applications.

## Chapter-2

### 2.1. Experimental technique

#### 2.1.1 Preparation of powder ceramic

For preparing barium strontium titanate by soft chemical route Barium Nitrate  $\text{Ba}(\text{NO}_3)_2$ , Strontium Nitrate  $\text{Sr}(\text{NO}_3)_2$ , Titanium dioxide ( $\text{TiO}_2$ ) and Oxalic acid ( $\text{COOH}$ )<sub>2</sub> were taken as precursors. 0.2M Barium nitrate, 0.2M strontium nitrate, 0.2M Titanium dioxide and 0.4M Oxalic acid water solutions were taken.

A 0.2molar barium nitrate solution was prepared by dissolving  $\text{Ba}(\text{NO}_3)_2$  in distilled water. Required amount of strontium nitrate was separately dissolved using minimum quantity of distilled water. Then strontium nitrate solution was drop-wise added to barium nitrate solution under constant stirring. A low concentration of barium nitrate solution must be used in order to avoid cations precipitation during this addition. A required amount of titanium dioxide ( $\text{TiO}_2$ ) was dispersed in 0.4M Oxalic acid solution in a separate vessel. The suspension was ultrasonic for 15min to break the soft agglomerates of the  $\text{TiO}_2$ . Now the barium and strontium nitrate mixed solution was added drop wise into the  $\text{TiO}_2$ -Oxalic acid suspension under vigorous stirring. Barium and Strontium-oxalate hydrates were precipitated inside the suspension by heterogeneous nucleation. Finally the pH of the suspension was adjusted to 7 by adding ammonium hydroxide solution. The precipitated mixture of  $\text{TiO}_2$  and barium strontium oxalate was separated by filtration and washed thoroughly using deionized water followed by drying at  $90^\circ\text{C}$  for 12hrs.

The decomposition behaviour of the resulting dried powder was studied using thermogravimetric analysis (TGA) and differential scanning calorimetry (DSC) using Netzsch STA 409C machine at a heating  $10^\circ\text{C}/\text{min}$  for room temperature upto  $1400^\circ\text{C}$ . Then the powder was calcined at  $1250^\circ\text{C}$  for 4hrs in air atmosphere to study the phase formation behaviour. The phase identification in powders was performed at room temperature using  $k_\alpha$  X-ray Diffractometer (PW-1830, Philips). The synthesized powder was pelletized at a pressure of 5tonns using polyvinyl alcohol as a binder. The pellets were sintered at  $1300^\circ\text{C}$  for 1hr in microwave

furnace. The microstructure of sintered specimen was studied using scanning electron microscopy (SEM). For dielectric measurement, the sintered pellet was electrode with silver conductive paste (Alpha Aesar). The frequency dependence of dielectric constant and loss tangent was obtained using a LCR meter in the frequency range from 1kHz to 1MHz at room temperature and the BaTiO<sub>3</sub> samples had measured temperature dependence study upto 200°C. The temperature was controlled with a programmable oven. All the dielectric data were collected while heating at a rate of 1°C/min.

### **2.1.2 Calcinations**

In this process the material is heated to a temperature below its melting point to effect the thermal decomposition or the phase transition other than melting point, or removal of a volatile fraction. Calcination is to be distinguished from roasting, in which more complex gas-solid reactions take place between the furnace atmosphere and the solids. Calcination reactions usually take place at or above the thermal decomposition temperature or the transition temperature (for phase transitions). This temperature is usually defined as the temperature at which the standard Gibbs free energy for a particular calcination reaction is equal to zero.

### **2.1.3 Sintering**

Sintering is a process of heating the material in a sintering furnace below its melting point until its particles adhere to each other. Sintering is traditionally used for manufacturing ceramic objects. When heat energy is applied to powder compact, the compact is densified and the average grain size is increases. Sintering makes the ceramic pure and maintains the uniformity in starting materials. This is process used to produced density control materials or compound from metal or ceramic powder by applying thermal energy. Sintering aims to produce sintered part with reproducible and if possible designed a microstructure through control the sintering variables.

## 2.2 Characterization

### 2.2.1 X-Ray Diffraction

X-ray diffraction is useful to describe crystallographic structure, chemical composition, and physical properties of materials and thin films. These techniques are based on observing the scattered intensity of an X-ray beam hitting a sample as a function of incident and scattered angle, polarization, and X-rays are electromagnetic radiation with typical photon energies in the range of 100 eV – 100keV. For diffraction applications, only short wavelength X-rays (hard X-rays) in the range of a few angstroms to 0.1 angstrom (1 keV - 120 keV) are used. Because the wavelength of X-rays is comparable to the size of atoms, they are ideally suited for probing the structural arrangement of atoms and molecules in a wide range of materials. The energetic X-rays can penetrate deep into the materials and provide information about the bulk structure.

$$2d\sin\theta = n\lambda$$

This is known as the Bragg's law, after W.L. Bragg, who first proposed it. In the equation,  $\lambda$  is the wavelength of the X-ray,  $\theta$  the scattering angle, and  $n$  an integer representing the order of the diffraction peak.

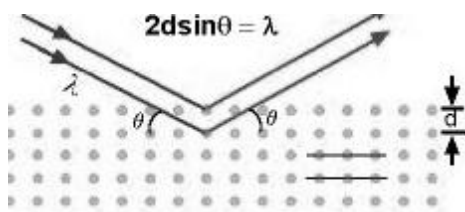


Fig. 3 X Ray Diffraction

### 2.2.2 Differential Scanning Calorimetry

DSC determines the temperature and heat of transformation. Unlike structural or microscopic methods of materials characterization, DSC can provide information on how a substance “got from here to there” during thermal processing. The basic principle for DSC is that, when the sample undergoes a physical transformation such as phase transition, more or less heat will be needed to flow to it than the reference to maintain both at the same temperature. Whether less or

more heat must flow to the sample depends on whether the process is exothermic or endothermic. For example, as a solid sample melts to a liquid it will require more heat flowing to the sample to increase its temperature at the same rate as the reference. This is due to the absorption of heat by the sample as it undergoes the endothermic phase transition from solid to liquid. Likewise, as the sample undergoes exothermic processes (such as crystallization) less heat is required to raise the sample temperature. By observing the difference in heat flow between the sample and reference. Properties measured by DSC include phase changes, glass transition, melting, purity, evaporation, sublimation, crystallisation, pyrolysis, heat capacity, polymerization, compatibility etc.

### **2.2.3 Thermogravimetry analysis**

In a thermogravimetric analysis the mass of the substance in a controlled atmosphere is recorded continuously as a function of temperature or time. As the temperature of the sample is increased, when the weights are plotted against temperature a curve characteristic of the substance is obtained. Such a curve is called a thermogravimetric curve or thermogram or thermal decomposition curve. Thermogravimetry provides information in a wide variety of chemical investigations some of these are 1.Calcination 2.Decomposition 3.Identification 4.Kinetics 5.Purity check 6.Thermal stability 7.Vaporization 8.Chemisorptions.

### **2.2.4 Scanning Electron Microscope (SEM)**

The scanning electron microscope (SEM) is used to study the surface morphology of the sample. It is an electron microscope and it takes the images of the surface of the samples by scanning it with a high-energy beam of electrons. The SEM can produce very high-resolution images of a sample surface, revealing details less than 1 nm in size. The SEM also produces images of high resolution, which means that closely spaced features can be examined at a high magnification. The electrons interact with the atoms that make up the sample producing signals that contain information about the surface of the sample topography, composition and other properties such as electrical conductivity.

### 2.2.5 Dielectric study

To measure the relative permittivity (dielectric constant) and dielectric loss, LCR meter can be used. In this work, (LCR Tester (Hioki, Japan, 42 Hz – 1MHz) were used to measure the dielectric constant and dielectric loss. The electroded samples were used to make the measurements. The LCR meter, was interfaced with the computer and the data (capacitance and  $D$  factor) was collected as a function of temperature at different frequencies. The measured capacitance was then converted into dielectric constant using the following formula:

$$C = \epsilon_0 \epsilon_r A/d$$

where,  $C$  : Capacitance in farad ( $F$ )

$\epsilon$  : Permittivity of free space in farad per meter ( $8.85 \times 10^{-12} F/m$ )

$\epsilon_r$  : Dielectric constant or relative permittivity of the sample.

$A$  : Area of each plane electrode in square meters ( $m^2$ )

$d$  : Separation between the electrodes in meters ( $m$ )

The study of dielectric properties is concerned with the storage and dissipation of electric and magnetic energy in materials. It is important to explain various phenomena in electronics, optics, and solid-state physics. A dielectric material is a substance that is a poor conductor of electricity, but an efficient supporter of electrostatic fields. If the flow of current between opposite electric charge poles is kept to a minimum while the electrostatic lines of flux are not impeded or interrupted, an electrostatic field can store energy. This property is useful in capacitors, especially at radio frequencies. Dielectric materials are also used in the construction of radio-frequency transmission lines.

## Chapter- 3

### 3.1 Result discussion

#### 3.1.1 DSC & TGA

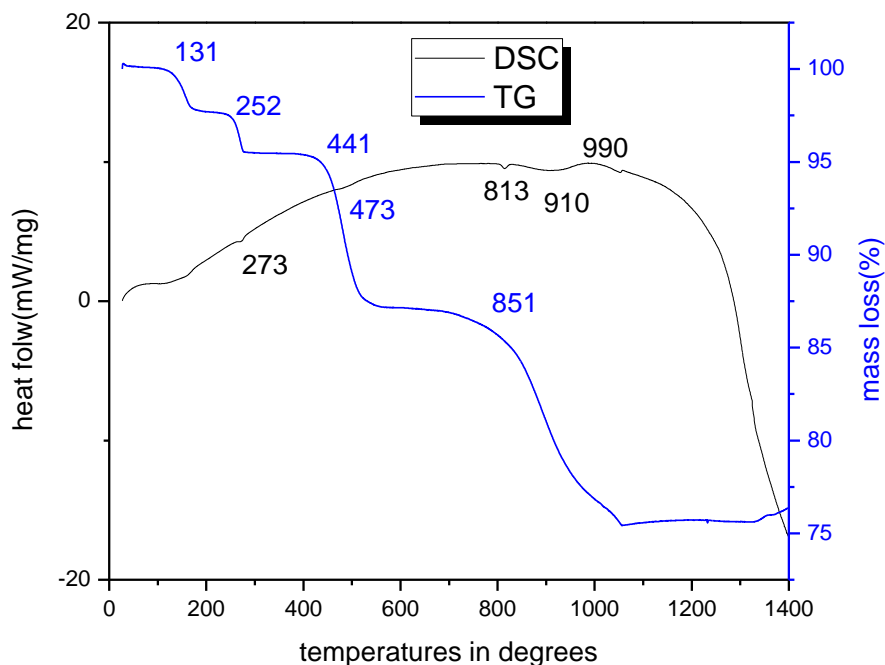
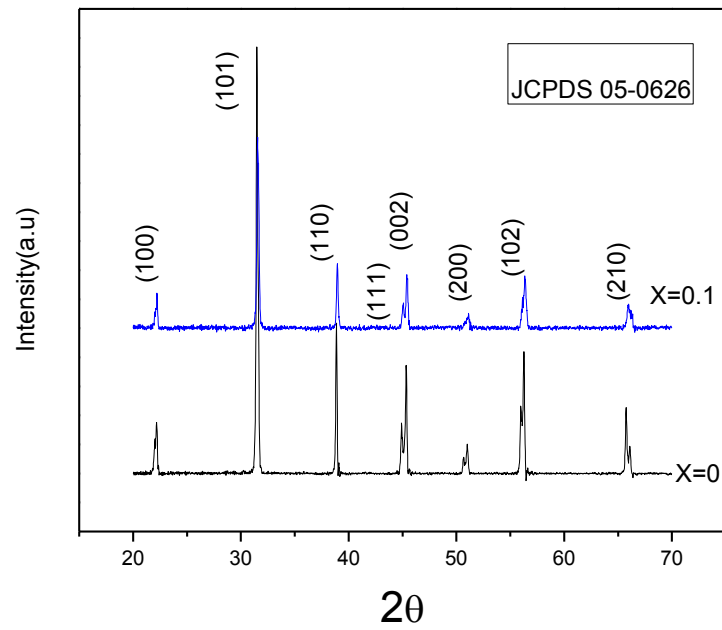


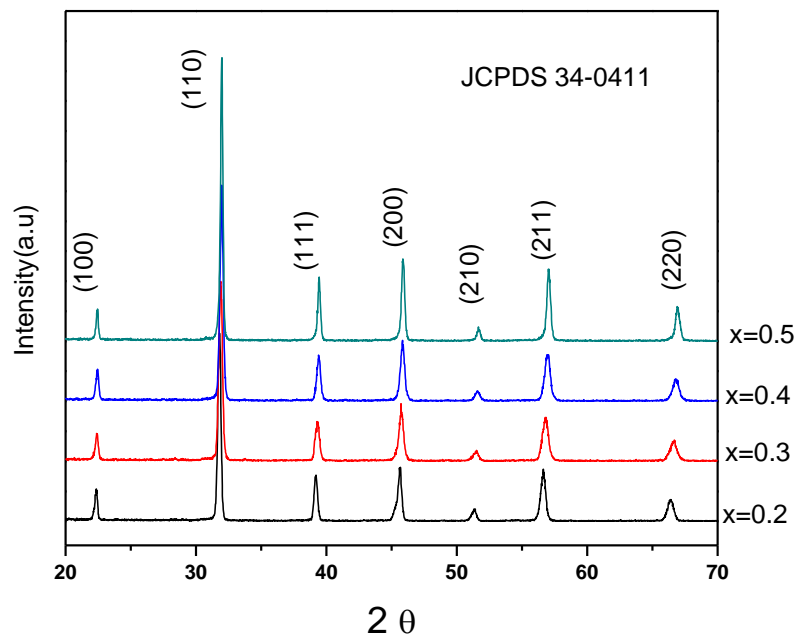
Fig4. TG and DSC plot of BaTiO<sub>3</sub>

The DSC and TG analysis of all the samples is carried out using differential scanning calorimetric and thermo gravitometric analysis by heating the sample at 10<sup>0</sup> C /min. The TG and DSC plots are shown in the Fig.. Here temperature is taken at X axis and mass loss and heat flow in Y axis. Endothermic peaks observed at 273<sup>0</sup>C, 813<sup>0</sup>C, 990<sup>0</sup>C temperatures. The peaks are not wider which corresponds that liquid phase not happened. TG plot of BaTiO<sub>3</sub> shows that at 473<sup>0</sup>C a broad mass loss occurs due to the evaporation of oxalic acid and at 851<sup>0</sup>C may be due to the loss of nitrate compounds. At 131<sup>0</sup>C and 252<sup>0</sup>C may be the loss of water molecules.

### 3.1.2 XRD



5(a)



5(b)

Fig 5.XRD pattern of Sr doped  $\text{BaTiO}_3$



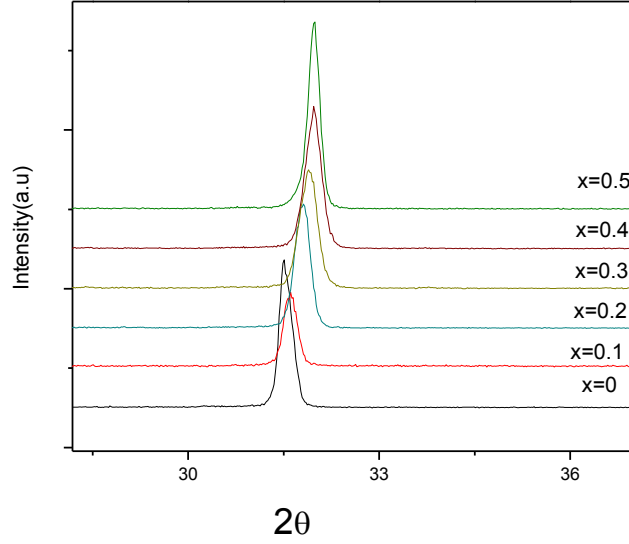


Fig 6.shows the peak shift of Sr doped BaTiO<sub>3</sub>

The Ba<sub>1-x</sub>Sr<sub>x</sub>TiO<sub>3</sub> polycrystalline samples were structurally characterized by X-ray diffraction. The patterns were recorded in a  $2\theta$  range from 20 to 70° in the  $2\theta$ - $\theta$  mode at room temperature using Cu K $\alpha$  radiation, presents the XRD patterns of BST samples calcined at 1250<sup>0</sup>C for 4 hrs with different Sr content  $x = 0.1$ - 0.5 with a increment of 0.1. The samples with large Sr concentration show a small shift in the XRD peaks towards larger  $2\theta$ . The shift increases with the increase in Sr content and corresponds to a decrease of the distances between the crystalline planes. When the Sr content increases the XRD data processing shows the decrease in the unit cell volume for BST samples which confirms that the Sr is incorporated in to BaTiO<sub>3</sub> matrix with out the presence of any deleterious phase. This effect, can be explained by the fact that the ionic radius of Sr<sup>2+</sup> is smaller than the ionic radius of Ba<sup>2+</sup>. The composition upto  $x=0.1$  shows tetragonal and higher concentration shows cubic structure. All patterns are well matched with the JCPDS 05-0626 and 34-0411 for tetragonal and cubic respectively. The matched hkl values are indicated in the figure. The lattice parameters are calculated using checkcell software and the values and all parameters are tabulated in the Table 1.

Table.1 Table of lattice parameter.

Conc(x)	Angle 2 $\theta$	FWHM	a=b	c	volume
X=0	31.4813	0.1440	3.9952	4.0341	64.39
X=0.1	31.5346	0.1440	3.9922	4.0193	64.06
X=0.2	31.8496	0.2880	3.9765	3.9765	62.83
X=0.3	31.8904	0.2160	3.9655	3.9655	62.37
X=0.4	31.9836	0.1200	3.9582	3.9582	61.96
X=0.5	31.9666	0.1920	3.9530	3.9530	61.77

### 3.1.3 SEM

The SEM micrographs show the uniform and circular well defined grains. The grain growth mechanism of Sr doped BaTiO<sub>3</sub> ceramics show that the grain size and porosity is depended on the doping concentration. The grain size decreases with increase in Sr concentration and also porosity is increased. This is because of the melting of Sr is higher than the Ba atom, so it requires more temperature to get the highly densed pellet.

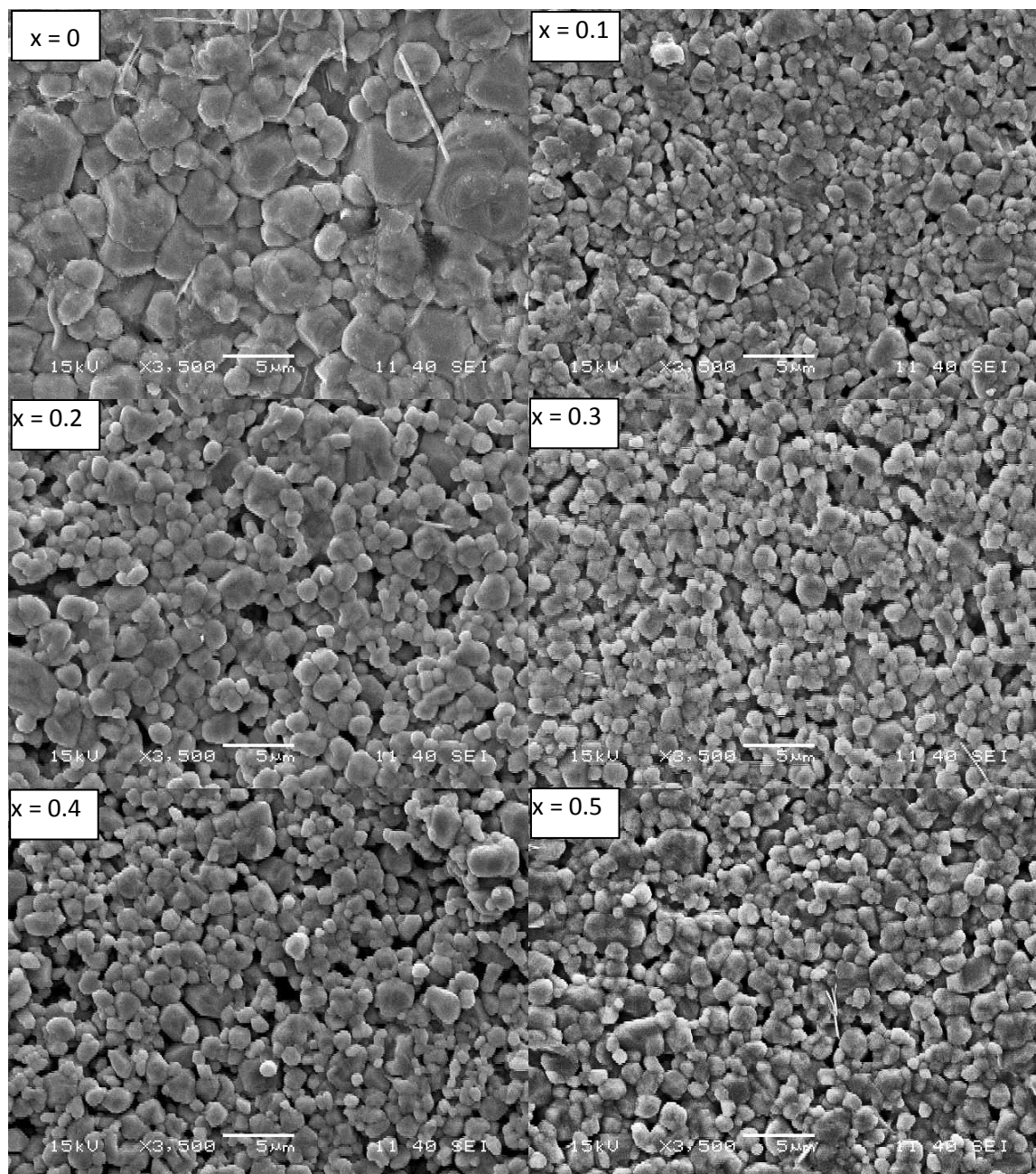
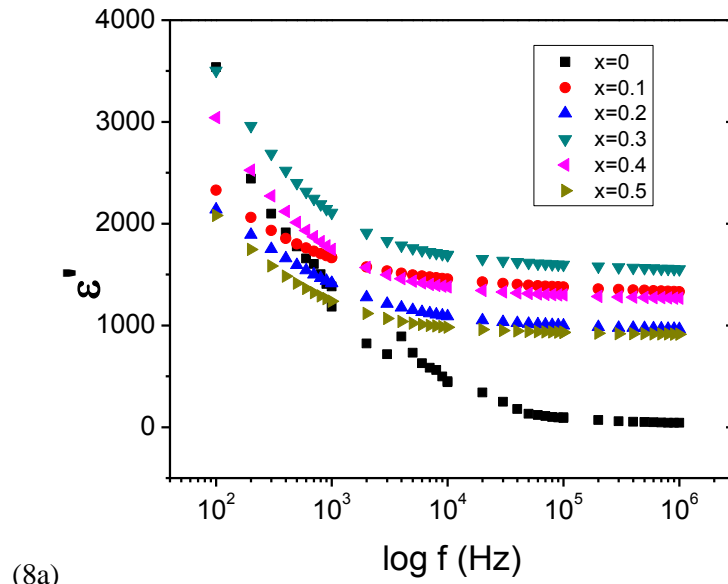


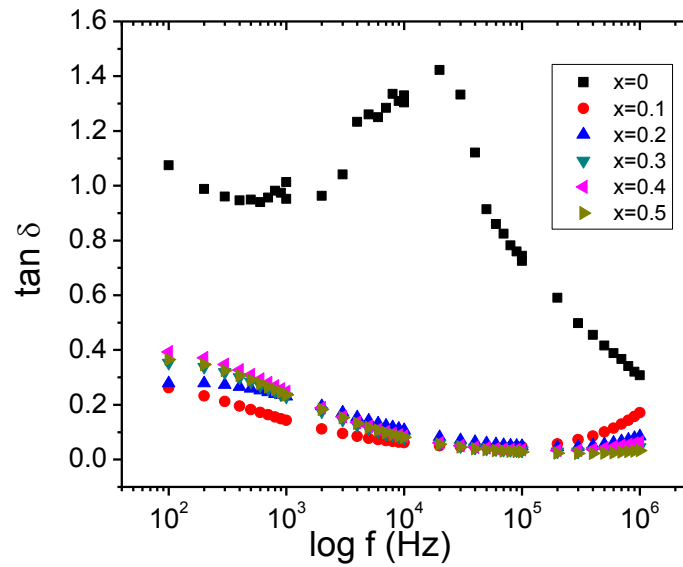
Fig7. SEM Images of Sr doped BaTiO<sub>3</sub>

#### 4.1.4 Dielectric study

##### Frequency dependence dielectric study



(8a)



(8b)

Fig8. Frequency dependence dielectric study of Sr doped BaTiO<sub>3</sub> at room temperature

The angular frequency  $\omega$  ( $=2\pi\nu$ ) dependence of the dielectric constant  $\epsilon'$  of BST for different compositions is shown in Fig8. The nature of the dielectric permittivity for free dipoles oscillating in an alternating field may be described in the following way. At very low frequencies ( $\omega \ll 1/\tau$ ,  $\tau$ =relaxation time), dipoles follow the field and we have  $\epsilon' = \epsilon_s$  (value of the dielectric constant at quasistatic fields). As the frequency increases (with  $\omega < 1/\tau$ ), dipoles begin to lag behind the field and  $\epsilon'$  slightly decreases. When frequency reaches the characteristic frequency ( $\omega = 1/\tau$ ), the dielectric constant drops (relaxation process). At very high frequencies ( $\omega \gg 1/\tau$ ), dipoles can no longer follow the field and  $\epsilon' \approx \epsilon_\infty$  (high-frequency value of  $\epsilon'$ ). Qualitatively this behavior has been observed in Fig(8a) BST (x=0) shows the higher dielectric constant at low frequency and less values at high frequency compared to all other doped samples. But BST (x=0.3) sample shows the higher dielectric constant among all the samples.

The loss tangent ( $\tan \delta$ ) is the ratio of the loss factor to the relative permittivity, and is a measure of the ratio of the electric energy lost to the energy stored in a periodic field. Fig (8b) shows the variation of dielectric loss with frequency at different temperatures. From the plots BST (x=0) it is clear that  $\tan \delta$  slightly increases first with frequency and then decreases at room temperature, it shows that the relaxation occurs at the room temperature in the experimental limits. But in the doped samples, the peak position is shifted to the very low frequency side. The higher dielectric loss that occurs at lower frequency is due to an accumulation of free charge. The polar ionization due to the charge accumulation decreases, leading to a decrease in the value of the dielectric loss.

## Temperature dependency dielectric study

Temperature dependence dielectric study is measured for various frequency to find out the transition temperature of the BST (x=0) samples. The measured peak shows that the transition temperature is at 147°C of all the frequencies. The value of  $\epsilon'$  increases gradually to a maximum value ( $\epsilon_m$ ) with increase in temperature and then decreases gradually indicating a phase transition. The maximum of dielectric permittivity,  $\epsilon_m$  and the corresponding temperature maximum  $T_m$ , depends upon the measurement frequency. An increase in the values of  $\epsilon_m$  at

lower temperature region may also be due to the increase in ionic conductivity resulting from the disordering of mobile cations in the oxygen octahedral skeleton.

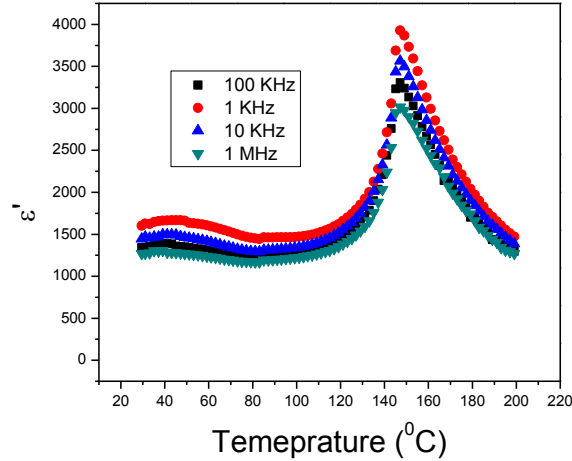


Fig9. Temperature dependence dielectric study of BaTiO<sub>3</sub>

Fig shows the frequency dependency permittivity of BST Ba<sub>1-x</sub>Sr<sub>x</sub>TiO<sub>3</sub> compositions. Permittivity of all the compositions was very stable in the frequency range 1KHz to about 1MHz. In general, permittivity( $\epsilon$ ) decreases with the increase in Sr concentration due to; (i) decrease in concentration of high permittivity material BaTiO<sub>3</sub> (ii) decrease in grain size resulting the in the decrease in the polarizability of the atoms in the structure. So it may be concluded from the study that the materials are suitable for the application in the frequency range 1KHz to about 1MHz.

Fig shows the frequency dependency of the dielectric loss of the samples. In general,  $\delta$  decreases with Sr substitution. At very low frequency, high dielectric loss is observed due to the presence of all types of polarization including space charge polarization. That also quickly decreases upto about 1MHz due to the space charge polarization. The dielectric loss of all the compositions was very stable in the frequency range 1KHz to about 1MHz. At high frequency, a dielectric loss peak is observed. Several possible cause exist for such dispersion including the hypothesis of the influence of the contact resistance between the probe and the electrode, resonance due to high dielectric constant. Figure 3 shows the temperature dependency of the permittivity of BaTiO<sub>3</sub> ceramic. The value of  $\epsilon'$  increases gradually to a maximum value ( $\epsilon_m$ ) with increase in

temperature and then decreases smoothly indicating a phase transition. The maximum of dielectric permittivity ( $\epsilon_m$ ) and the corresponding temperature maximum ( $T_m$ ) depend upon the measurement frequency for all the compositions.

### 3.1.5 PE loop

All the sintered samples are measured Electric field versus Polarisation by P-E loop tracer with applying DC field. From the PE loop tracer, all parameters ( $E_c$ ,  $P_s$ ,  $P_r$ ) are measured and inserted in the figures. By getting the loop, it is confirmed the materials are ferroelectric materials.

Table2.  $E_c, P_s, P_r$  values of  $x=0, 0.1, 0.2, 0.4$ ,

Con(X)	$E_{max}(kv/cm)$	$E_c(kv/cm)$	$P_s(\mu C/cm^2)$	$P_r(\mu C/cm^2)$
X=0	3.347	0.847	1.542	0.273
X=0.1	12.157	3.243	4.774	1.649
X=0.2	3.648	0,721	1.052	0.207
X=0.4	8.355	2.731	2.249	0.792

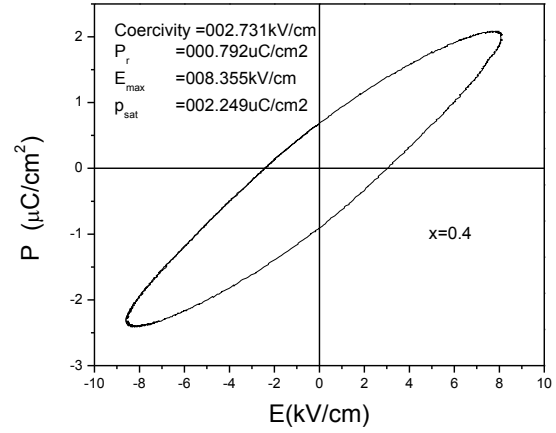
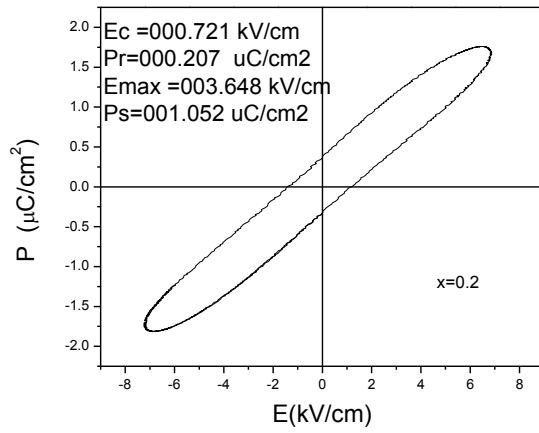
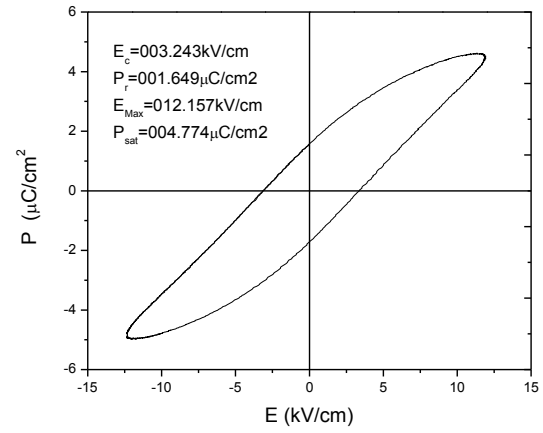
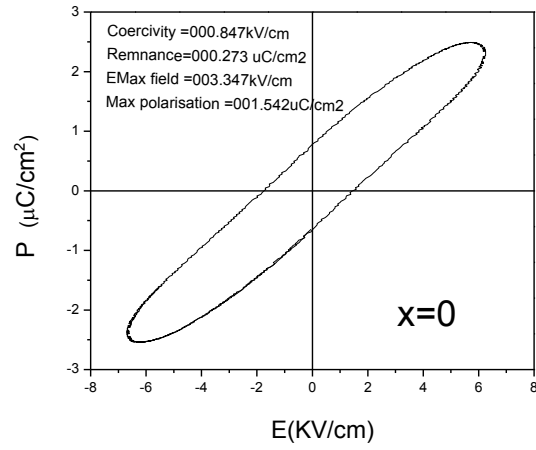


**Fig10.** shows the PE loop of Sr doped BaTiO<sub>3</sub> ceramics at room temperature



## Chapter 4

### Conclusion

Single Phase Sr doped Barium Titanate ( $\text{Ba}_{1-x}\text{Sr}_x\text{TiO}_3$ ) powder was prepared by soft chemical route.

- The XRD study shows that for  $x=0$  and  $x=0.1$  tetragonal structure and for higher doping showing cubic structure.
- The SEM micrograph shows that the grain size is affected by the doping concentration.
- The dielectric study shows that the materials are showing high dielectric constant value showing normal ferroelectric behavior.
- The P-E loop study shows that material is showing ferroelectric behavior.

## References

- 1.L. L. Hench and L. K. West, Principles of Electronic Ceramics, (John Wiley & Sons,Inc., 1990), pp244-247.
- 2.Goldschmidt, V. M., “Skifter Norske Videnskaps-Akad,” Oslo, I: Mat. - Naturv. Kl., 2, 8 (1926).
- 3.Bernard Jaffe, William R. Cook, Jr., and Hans Jaffe, Piezoelectric Ceramics, (Academic Press Limited, 1971), pp49-51. *ibid*, p50.
- 4.A. J. Moulson and J. M. Herbert, Electroceramics, (Chapman displacements of atoms that lead to the distortion of the structure and the reduction of symmetry have profound effects on physical properties, perovskite structure materials play such an important role in dielectric ceramic.
- 5.H. T. Martirena and J. C. Burfoot, *Ferroelectrics* 7, 151–152 (1974).
- 6.A.J.Burggraaf, Proc.9th Int Cong.on Sci of Ceramics, Noordwijkerhout, Netherland (1977).
7. C.G.F Stenger, A.J.Burggraaf, *J.Phys. Chem.Solids*, 41, 25 (1980), W. Kanzig, *Helv. Phys. Acta* 24, 175 (1951).
8. W. Kanzig, *Ferroelectric and Antiferroelectrics*, Academic Press, New york (1957).
9. J. Fritesberg, Proc. 4th Int. Meeting on Ferroelectricity, Leningrad (1977).
- 10.A.Chakrabarti et al./*physica B* 404(2009) 1498-1502